

# Accuracy of a 3D printed sleeveless guide system used for fiber post removal: An *in vitro* study

Siyi Mo<sup>a,1</sup>, Yongwei Xu<sup>b,1</sup>, Lei Zhang<sup>a</sup>, Ye Cao<sup>a</sup>, Yongsheng Zhou<sup>a</sup>, Xiaoxiang Xu<sup>a,\*</sup>

<sup>a</sup> Department of Prosthodontics, Peking University School and Hospital of Stomatology, National Center of Stomatology, National Clinical Research Center for Oral Diseases, National Engineering Research Center of Oral Biomaterials and Digital Medical Devices, Beijing Key Laboratory of Digital Stomatology, Research Center of Engineering and Technology for Computerized Dentistry Ministry of Health, NMPA key Laboratory for Dental Materials, Zhongguancun South Avenue 22, Beijing 100081, China

<sup>b</sup> Department of dentistry, Peking University People's Hospital, Xizhimen South Street 11, Beijing 100044, China

## ARTICLE INFO

### Keywords:

Guided technique  
3D printing  
Dental root post  
*In vitro* study  
Computer-aided design

## ABSTRACT

**Objectives:** The removal of fiber post is often a challenging task. A 3D printed assembled sleeveless system that guides the head of the handpiece instead of the drill was developed to address this issue. This study aimed to evaluate the accuracy of this novel guide system using an *in vitro* approach.

**Methods:** A standard maxillary typodont was digitized. The right first molar, the right central incisor, the left first premolar, and the left second molar in the digitized dentition were virtually crown-amputated. Four cylinders (diameter: 6 mm, height: 12 mm) were positioned along the directions of the main roots of these teeth to establish the virtual test model. Ten copies of the test model were printed using light-polymerizing resin. Four assembled sleeveless guide systems targeting the cylindrical axes were designed and printed using titanium alloy. One senior prosthodontist performed the drilling task targeting each cylindrical axis aided by the guide system or freehand (20 teeth each). The drilled models were scanned. The coordinates of the centers of all perforations and circular bases on the coronal and apical surfaces were obtained. The linear and angular deviations between the actual drilling path and the cylindrical axis for each tooth were calculated and analyzed.

**Results:** The guided group exhibited significantly smaller linear and angular deviations than the freehand group (coronal linear deviation:  $0.19 \pm 0.09$  mm vs.  $0.35 \pm 0.18$  mm,  $p = 0.0012$ ; apical linear deviation:  $0.54 \pm 0.19$  mm vs.  $1.71 \pm 0.51$  mm,  $p < 0.001$ ; angular deviation:  $2.67 \pm 1.07^\circ$  vs.  $8.48 \pm 2.86^\circ$ ,  $p < 0.001$ ).

**Conclusion:** The accuracy of the 3D printed assembled sleeveless guide system used for fiber post removal is superior to that of the freehand method within the limits of an *in vitro* design.

**Clinical significance:** For the removal of fiber posts, the present 3D printed sleeveless guide system can provide better accuracy than the conventional freehand method. This may justify the diffusion of the guided technique for fiber post removal.

## 1. Introduction

Fiber posts are widely applied for the reconstruction of endodontically-treated defective teeth with ideal mechanical properties, superior optical qualities, and reliable clinical prognosis [1]. However, in cases with recrudescence periapical infections, the removal of fiber posts for endodontic revision has become a challenging task, particularly for general practitioners. Although various tools were introduced to remove fiber posts (e.g., dental operating microscope, ultrasonic working tip or special post removal drill kit) [2–4], risks of root

perforation, axis deviation, dentin loss and consequent fragilization of the roots still exist [5–8]. Therefore, considerable chairside time, meticulous manual operation, and sufficient endodontic experience are required in such cases to prevent poor tooth prognosis.

With the rapid development of digital technologies in dentistry, such as three-dimensional (3D) data acquisition, computer-aided design (CAD), and computer-aided manufacturing (CAM) [9], guided implantology and endodontics have emerged [10,11]. These guided techniques adopt the combined data from cone-beam computed tomography (CBCT) and optical scans to design the optimal virtual path. The design

\* Corresponding author.

E-mail address: [xiaoxiang86@bjmu.edu.cn](mailto:xiaoxiang86@bjmu.edu.cn) (X. Xu).

<sup>1</sup> These authors contributed equally to this work.

information is then transferred to a preformed sleeve structure that is integrated into an individualized CAM/3D printed guide template which facilitates the intraoral operation with greater accuracy, safety, and efficiency compared to the traditional freehand method [10,11]. Recently, the guided technique has also been applied in the removal of fiber posts, providing a new strategy to address the challenges of post removal [12–15]. Nevertheless, for fiber post removal, there were some limitations of the traditional design that guides the drills with dedicated sleeves. First, specific cylindrical drills with appropriate diameters and lengths are required. In many circumstances, it is difficult to find suitable drills, especially for teeth with multi-canals, which makes the guided technique impractical. Moreover, the sleeve used in the guide occupies additional space, which restricts its application in the distal region with limited vertical height. Also, the traditional guide with a sleeve covers the operative field, which impedes irrigation and visibility during the drilling process, leading to potential thermal damage to surrounding tissues [16] and inability to evaluate the deviation in real time. These disadvantages impede application of the guided technique for fiber post removal.

To address these challenges, we developed a novel 3D printed assembled sleeveless guide system that guides the head of the handpiece instead of the drill through assembly structures with the aid of an adapter. The sleeveless design can enable flexible drill use strategy for fiber post removal, facilitate operation in the limited posterior region, avoid drill abrasion against the sleeve, and achieve good visibility of the operative field. The assembled design can increase the coverage area over the dentition and permit extension into undercut areas, which improves stability without impacting the insertion. Therefore, the novel guide system can be applied in almost all clinical situations that require fiber post removal with better clinical practicability and flexibility. However, the accuracy of this assembled sleeveless guide system has not been investigated, and this is essential for its clinical application.

This study aimed to evaluate the accuracy of this assembled sleeveless guide system for fiber post removal using an *in vitro* approach. The null hypothesis was that the accuracy of drilling with 3D printed assembled sleeveless guide system was equivalent to freehand drilling.

## 2. Materials and methods

A pilot study was conducted before the study in order to verify the methodology and calculate the sample size. A total sample size of 40 was calculated using G\*Power 3 [17] to detect a significant difference with 80% power based on the study design.

### 2.1. Model preparation

A standard maxillary jaw typodont (Basic models, Nissin Dental Products, Kyotoshi, Kyoto, Japan) was digitized (TRIOS 3, 3Shape, Copenhagen, Denmark) and imported to a dental CAD software (DentalCAD, Exocad GmbH, Darmstadt, Germany). The right first molar, the right central incisor, the left first premolar, and the left second molar of the maxillary dentition were virtually crown-amputated, with 1–1.5 mm high cervical part left. A digital model entity (thickness: 2 mm) was built with a hollow base (height: 5–20 mm) and the new data was imported to a reverse engineering software (Geomagic Studio, 3D Systems, Rock Hill, SC, USA). The virtual model was separated horizontally into two parts. The upper section was used as the experimental model and comprised the dentition and 2–4 mm of the gingiva. The lower section included mainly the hollow base with a uniform height of approximately 10 mm and was enclosed with a 5 mm high solid floor to support the experimental model. Four cylinders (diameter: 6 mm, height: 12 mm) were generated and positioned along the directions of the main root canals of the corresponding crown-amputated teeth, with a 1–3 mm high exposed section above the residual teeth, ensuring no contact with the inner wall of the hollow base (Fig. 1A,B). Two matched convex–concave structures were added to the distal surface of the upper and lower parts to facilitate their alignment (Fig. 1C). The data of the experimental model and base were sent to a 3D printer (Objet 260, Stratasys, Eden Prairie, MN, USA). Ten copies of experimental model and one copy of the model base were printed using light-polymerizing resin (MED 690, Stratasys) (Fig. 1D).

### 2.2. Guide preparation

The guide stents (thickness: 1.5 mm) for each targeted cylinder were

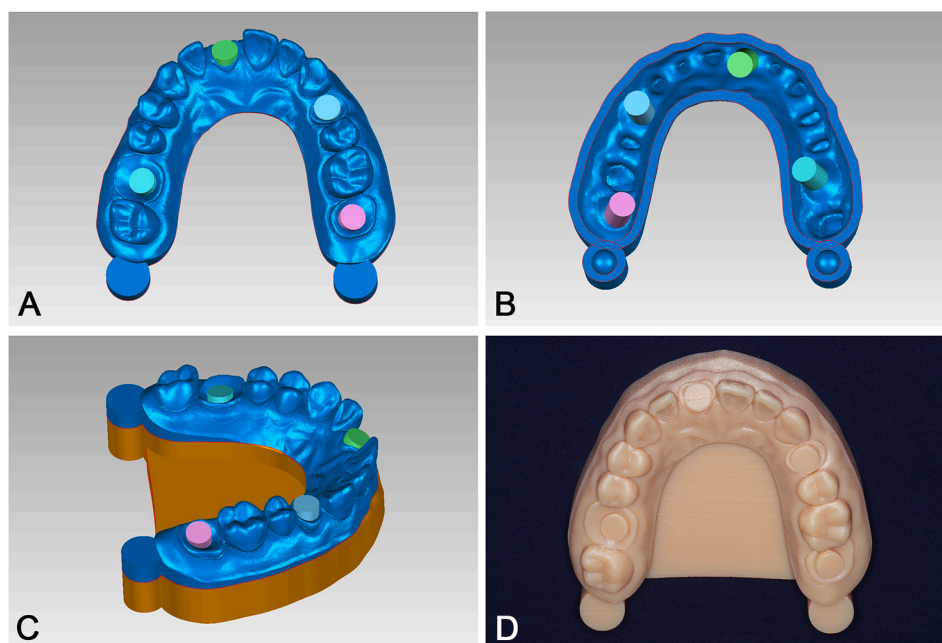


**Fig. 1.** Design and manufacture of experimental model and base. (A) Top view of the designed experimental model; (B) Bottom view of the designed experimental model; (C) Designed experimental model inserted on the base; (D) Printed experimental model inserted on the base.

designed using the splint module of the dental CAD software (Dental-CAD, Exocad GmbH), which covers three to six neighboring teeth according to the targeted tooth position. The stent data were imported to the reverse engineering software (Geomagic Studio, 3D Systems). The guide tube (inner diameter: 13.85 mm; thickness: 1.5 mm) with the concentric axis of each cylinder was generated and split into three parts to form the inspection window and passage for the dental handpiece. The guide stents were separated into two parts along the central line of the occlusal surface with a 1 mm gap width. The matched lock components including pin and jack structures were formed and placed at the mesial and distal sides of each stent. The separate parts of the guide tube, stent, and lock component on the same side were combined (Fig. 2). In addition, a cylindrical adaptor (outer diameter: 13.7 mm) was generated according to the surface configuration of the head of a contra-angle

electric handpiece (CA 1:1 Standard, Bien Air Medical Technologies, Bienne, Switzerland) acquired by a chairside scanner (TRIOS 3, 3Shape) (Fig. 3). The data of all components of the assembled sleeveless guide system and the adaptor were sent to a metal 3D printer (M2, Concept Laser GmbH, Lichtenfels, Germany) and printed using titanium alloy material (Titanium for Medicals, Optimal Material Technology, Chengdu, China) (Fig. 4).

### 2.3. Data acquisition

The model base was attached to a dental simulator (NISSIM type 2, Nissin Dental Products) with a magnetic plate adhered to it. The experimental models were randomly divided into a guided group and a freehand group. The drilling task targeting the central axis of each cyl-

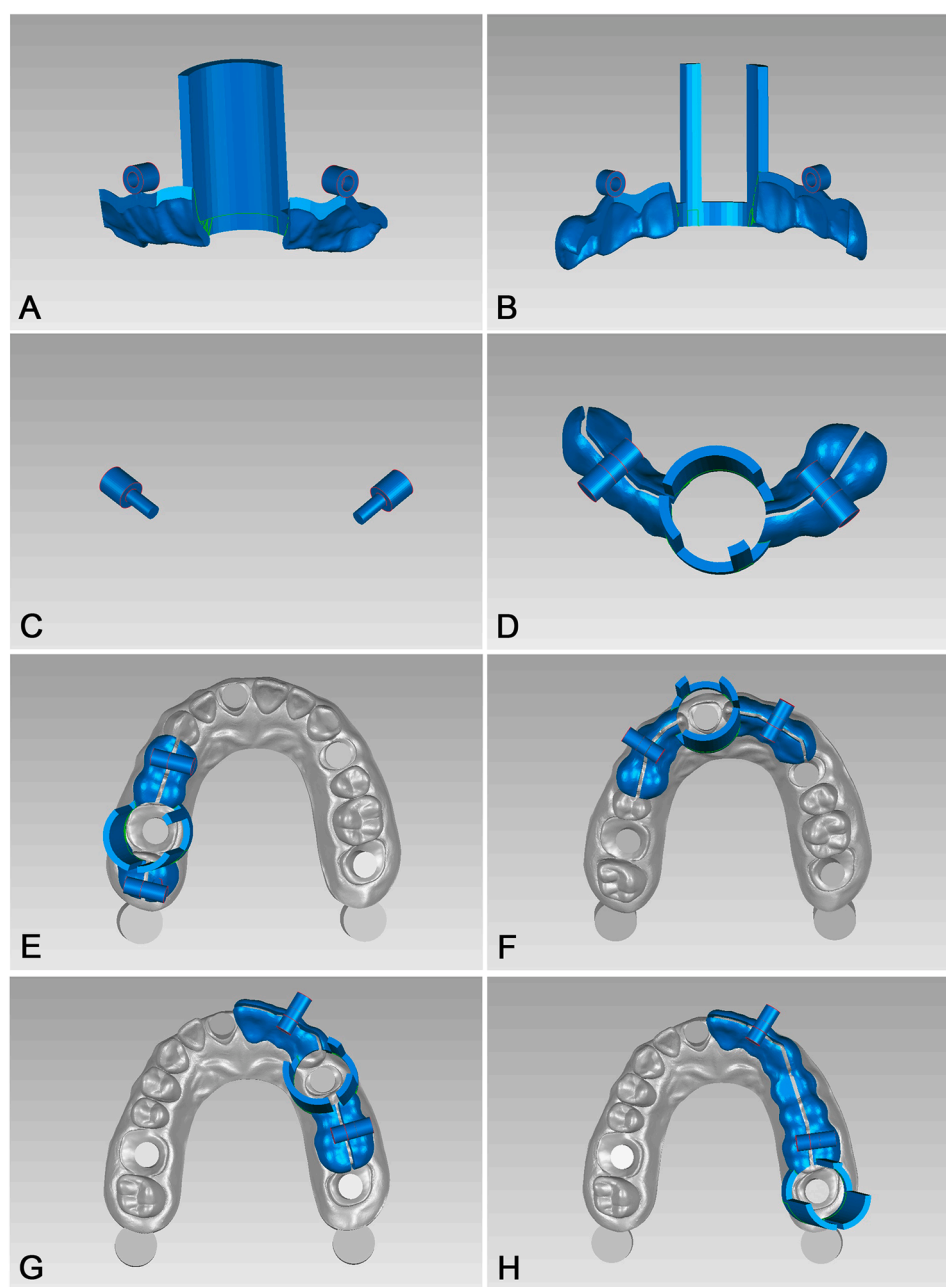


**Fig. 2.** Design procedure of the assembled sleeveless guide system. (A) Palatal part of guide system; (B) Labial part of guide system; (C) Pin structures at the two sides; (D) Assembled guide system; (E) Guide system for the right first molar; (F) Guide system for the right central incisor; (G) Guide system for the left first premolar; (H) Guide system for the left second molar.

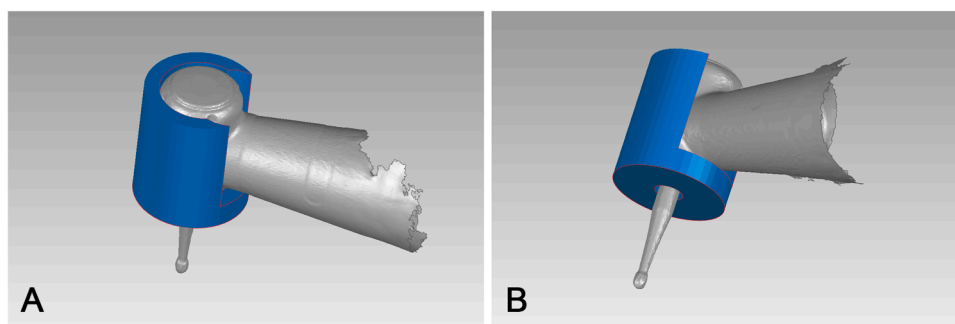


Fig. 3. Designed adaptor. (A) Top side view of the adaptor of electric handpiece; (B) Bottom side view of the adaptor of electric handpiece.

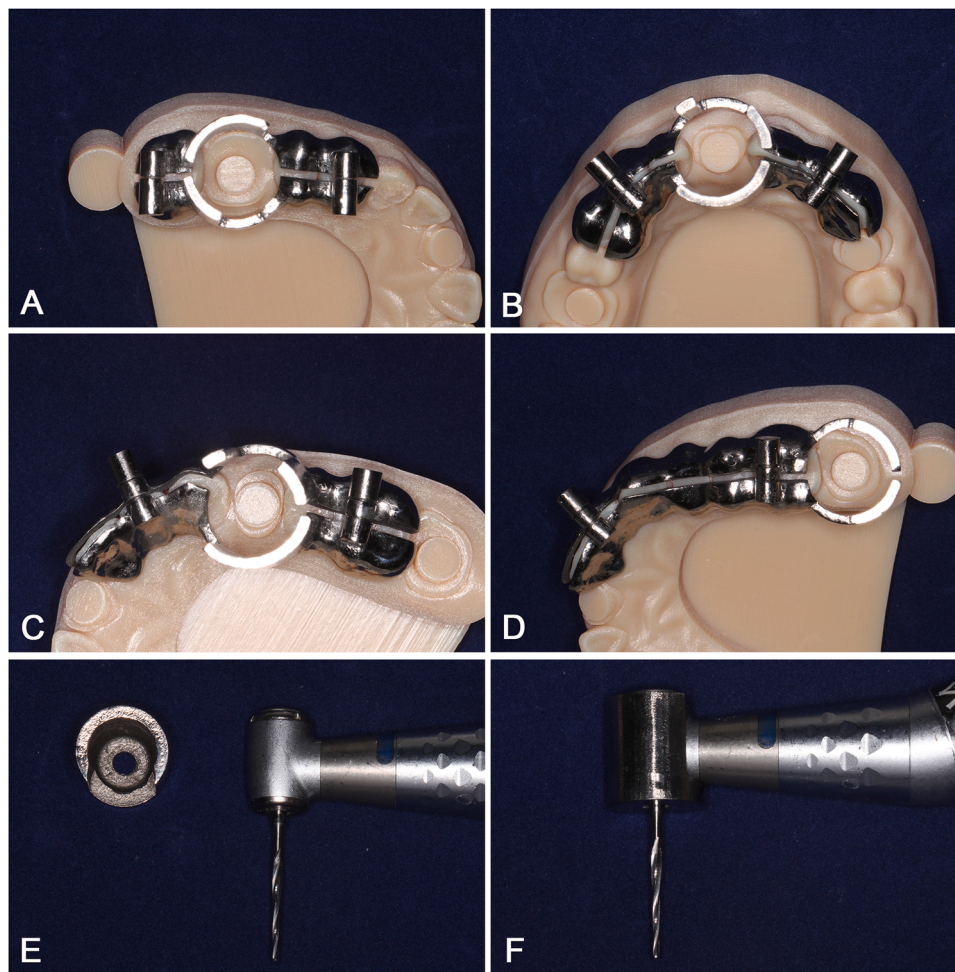


Fig. 4. Printed guide system and adaptor. (A) Printed guide system for the right first molar; (B) Printed guide system for the right central incisor; (C) Printed guide system for the left first premolar; (D) Printed guide system for the left second molar; (E) Top view of printed adaptor placed near the handpiece. (F) Printed adaptor inserted on the handpiece.

inder was then conducted by one senior prosthodontist with application of the guide system or freehand according to the exposed cylinder above the residual tooth (20 teeth each). A taper tungsten carbide drill with working length 21.5 mm (Reaccess Kit, RTD, Saint Egrève, France) installed on the contra-angle electric handpiece (CA 1:1 Standard, Bien Air Medical Technologies) with the adaptor was used to drill through the entire cylinder. The operator was not allowed to check the result during the drilling task to avoid the learning effect and maintain consistency among repeated operations. Then, each drilled experimental model was scanned to capture the entire surface configuration, including the top and bottom as a whole (TRIOS 3, 3Shape). The data were analyzed using

Geomagic Studio. The geometrical centers of all perforations and circular bases of the cylinders were defined by the feature detection function and the 3D coordinates of each point were acquired (Fig. 5). The linear deviation between the center of the perforation and cylindrical base at the coronal and apical surfaces, as well as the angular deviation between the actual drilling axis and the cylindrical axis, were calculated according to the rules of analytic geometry as follows:

$$\text{Linear deviation } A'-A = \sqrt{(x_{A'} - x_A)^2 + (y_{A'} - y_A)^2 + (z_{A'} - z_A)^2}$$

$$\text{Linear deviation } B'-B = \sqrt{(x_{B'} - x_B)^2 + (y_{B'} - y_B)^2 + (z_{B'} - z_B)^2}$$

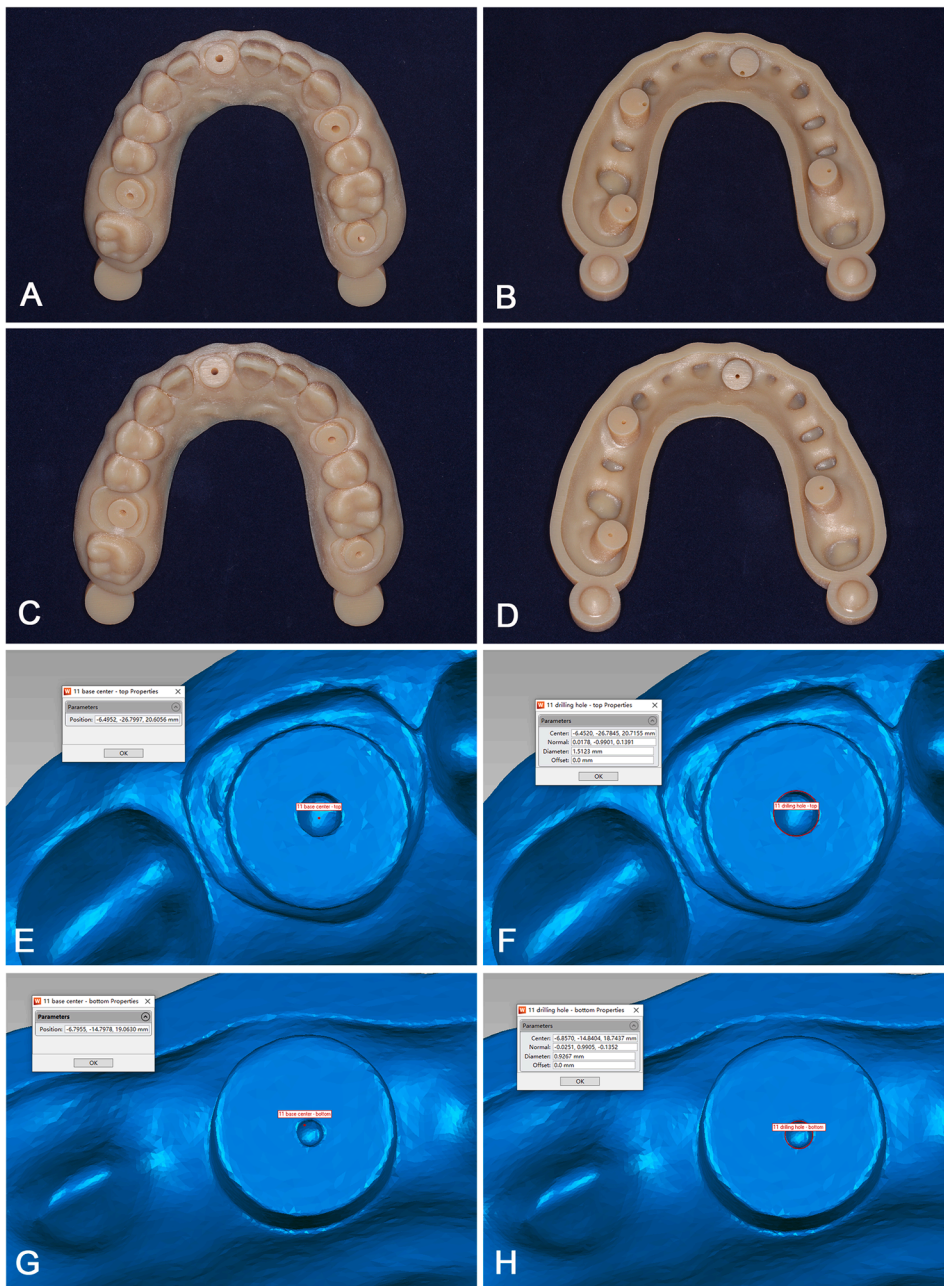


**Fig. 5.** Drilled experimental models and acquisition of 3D coordinates of geometrical centers based on the scanned experimental models. (A) Top view of the experimental model drilled freehand; (B) Bottom view of the experimental model drilled freehand; (C) Top view of the experimental model drilled with guide; (D) Bottom view of the experimental model drilled with guide; (E) Coordinates of the center of coronal circular base; (F) Coordinates of the center of the coronal perforation; (G) Coordinates of the center of apical circular base; (H) Coordinates of the center of the apical perforation.

**Angular deviation  $\theta$ :**

$$\vec{AB} : (x_B - x_A, y_B - y_A, z_B - z_A)$$

$$\vec{A'B'} : (x_{B'} - x_{A'}, y_{B'} - y_{A'}, z_{B'} - z_{A'})$$

$$\vec{AB} \cdot \vec{A'B'} = (x_B - x_A) \times (x_{B'} - x_{A'}) + (y_B - y_A) \times (y_{B'} - y_{A'}) + (z_B - z_A) \times (z_{B'} - z_{A'})$$

$$|\vec{AB}| = \sqrt{(x_B - x_A)^2 + (y_B - y_A)^2 + (z_B - z_A)^2}$$

$$|\vec{A'B'}| = \sqrt{(x_{B'} - x_{A'})^2 + (y_{B'} - y_{A'})^2 + (z_{B'} - z_{A'})^2}$$

$$\theta = \cos^{-1} \left( \frac{\vec{AB} \cdot \vec{A'B'}}{|\vec{AB}| \times |\vec{A'B'}|} \right) \times \frac{180}{\pi}$$

Note: A ( $x_A, y_A, z_A$ ), center of the circular base of the coronal surface; A' ( $x_{A'}, y_{A'}, z_{A'}$ ), center of the perforation of the coronal surface; B ( $x_B, y_B, z_B$ ), center of the circle base of the apical surface; B' ( $x_{B'}, y_{B'}, z_{B'}$ ), center of the perforation of the apical surface.

**2.4. Statistical analyses**

Statistical analyses were performed using SPSS v20.0 (IBM Corp, Chicago, IL, USA). The normality of data distribution was evaluated using the Shapiro-Wilk test. Differences in the deviation results of the two groups and between four tooth positions were analyzed using two-way analysis of variance. Differences of the overall deviation results

between the guided and freehand groups were compared using 2-sided t-test with Welch's correction. Descriptive statistics including mean, standard deviation and 95% confidence intervals were calculated for both groups. A value of  $p < 0.05$  was considered statistically significant.

### 3. Results

Regarding coronal linear, apical linear, and angular deviations, no significant main effect of the tooth position factor or interaction effect (tooth position X group) was detected ( $p > 0.05$ ), but there was a significant main effect of the group factor ( $p < 0.01$ ). The means  $\pm$  standard deviations of the linear and angular deviation data for the two groups and four tooth positions are presented in Table 1.

Compared with the freehand group, the guided group exhibited significantly lower overall coronal linear deviation ( $0.19 \pm 0.09$  mm vs.  $0.35 \pm 0.18$  mm,  $t = 3.609$ ,  $p = 0.0012$ ), apical linear deviation ( $0.54 \pm 0.19$  mm vs.  $1.71 \pm 0.51$  mm,  $t = 9.552$ ,  $p < 0.001$ ), and angular deviation ( $2.67 \pm 1.07^\circ$  vs.  $8.68 \pm 2.46^\circ$ ,  $t = 10.01$ ,  $p < 0.001$ ). The means  $\pm$  standard deviations and 95% confidence intervals of all linear and angular deviation data for the two groups are summarized in Table 2.

### 4. Discussion

The present study used an *in vitro* approach to assess the accuracy of a 3D printed assembled sleeveless guide system for fiber post removal. The results revealed that the accuracy of drilling with this guide system was significantly higher than that of the freehand method. Therefore, the null hypothesis was rejected.

Regarding fiber post removal under clinical conditions, the initial drilling point at the top of the fiber post is always visible; hence, the coronal linear deviation is not of concern for the real operation. The angular deviation is the most important result for clinical consideration. The guided group in this study exhibited an average angular deviation of  $2.67 \pm 1.07^\circ$ . Although the traditional guide system with sleeve was not applicable in our study or in circumstances using taper drills, the comparison can be made based on independent results reported in other *in vitro* studies. Su et al. investigated the accuracy of access cavity preparation via a guided endodontics technique and reported the angular

**Table 1**  
Linear and angular deviations for different targeted teeth in the freehand and guided groups.

		16#	11#	24#	27#	Statistics
Coronal deviation (mm)	Freehand	0.42 $\pm$ 0.23	0.34 $\pm$ 0.13	0.28 $\pm$ 0.19	0.38 $\pm$ 0.18	$F_{\text{position}}(3,32) = 0.589$ ,
	Guide	0.20 $\pm$ 0.09	0.12 $\pm$ 0.07	0.25 $\pm$ 0.04	0.20 $\pm$ 0.12	$p_{\text{position}} = 0.626$
	Statistics	$F_{\text{group}}(1,32) = 12.64$ , $p_{\text{group}} = 0.001$				
Apical deviation (mm)	Freehand	1.49 $\pm$ 0.29	1.94 $\pm$ 0.56	1.94 $\pm$ 0.52	1.47 $\pm$ 0.56	$F_{\text{position}}(3,32) = 0.599$ ,
	Guide	0.62 $\pm$ 0.33	0.46 $\pm$ 0.09	0.48 $\pm$ 0.14	0.60 $\pm$ 0.13	$p_{\text{position}} = 0.620$
	Statistics	$F_{\text{group}}(1,32) = 96.39$ , $p_{\text{group}} < 0.001$				
Angular deviation ( $^\circ$ )	Freehand	7.99 $\pm$ 1.41	9.99 $\pm$ 3.28	9.67 $\pm$ 2.59	7.10 $\pm$ 1.49	$F_{\text{position}}(3,32) = 0.701$ ,
	Guide	2.60 $\pm$ 1.68	2.47 $\pm$ 0.29	2.19 $\pm$ 0.71	3.43 $\pm$ 1.00	$p_{\text{position}} = 0.559$
	Statistics	$F_{\text{group}}(1,32) = 110.7$ , $p_{\text{group}} < 0.001$				

16#: right first molar; 11#: right central incisor; 24#: left first premolar; 27#: left second molar.

**Table 2**

Means  $\pm$  standard deviations and 95% confidence intervals of the overall linear and angular deviations of the freehand and guided groups.

		Freehand	Guided	p-value
Coronal linear deviation (mm)	Mean $\pm$ SD	$0.35 \pm 0.18$	$0.19 \pm 0.09$	0.001
	95% CI	0.27–0.44	0.15–0.23	
	Mean $\pm$ SD	$1.71 \pm 0.51$	$0.54 \pm 0.19$	<0.001
Apical linear deviation (mm)	95% CI	1.47–1.95	0.45–0.63	
	Mean $\pm$ SD	$8.68 \pm 2.46$	$2.67 \pm 1.07$	<0.001
	95% CI	7.53–9.84	2.17–3.18	

SD: standard deviation; CI: confidence intervals.

deviation was  $2.8 \pm 2.6^\circ$  [18]. A meta-analysis by Bover-Ramos et al. summarized the accuracy of implant placement with computer-guided surgery and revealed an angular deviation of  $2.39 \pm 0.35^\circ$  for eight *in vitro* studies [19]. Considering the successful clinical application of guided technique in endodontics [20] and implantology [21], a similar angular deviation generated using this sleeveless guide system appears clinically acceptable. It is noteworthy that an open-frame sleeveless guided system has been reported recently in the field of implant dentistry with reliable clinical performance, further supporting the feasibility of the sleeveless principle [22]. The novel sleeveless system guided the head of the handpiece instead of the drill; therefore, the distance between the guide tube and the working end of the drill is longer than that of the traditional guide design with sleeve. The results presented confirm that this factor does not influence accuracy of the guide system. The new sleeveless design can provide unrestricted drill selection and clear operation visibility, and save the additional space of the sleeve structure, thus exhibiting better clinical practicability and flexibility for fiber post removal compared with the traditional sleeve design. The apical linear deviation is positively related to the length of the drilling path. In this study, the height of the cylinder was 12 mm, which is longer than the length of fiber posts in most clinical cases. Thus, the mean apical linear deviation of  $0.54 \pm 0.19$  mm in this study should be interpreted considering the height of the cylinder and not referred to clinical settings directly. The coronal and apical linear deviations in this study were all horizontal deviations. Vertical deviation was not included in this study since it is not clinically critical for fiber post removal. Based on the present results, the accuracy of drilling was not affected by different distributions of targeted teeth, including the free end form for the second molar. This suggests that the various guide designs corresponding to different tooth positions do not impact the accuracy of this guide system.

Several factors that may contribute to the deviations are identified. The first is the gap between the inner side of the guide tube and the outer surface of the adaptor, which may cause potential axial deflection of the head of the handpiece. This gap cannot be removed but only be reduced for the required passage. We reduced the gap width to 0.15 mm based on practical manufacturing precision. Future improvements of the 3D printing technique should enable this gap to be reduced further. In addition, the angular deviation can be corrected in real time during the operation, by examining the parallel alignment between the drill and the tube through the inspection window of the guide system. The other factor that may contribute to the deviations is the stability of the guide template on the dentition. Although this novel assembled guide design improved the stability by the enlarged coverage area and the allowance for undercut entry compared with the traditional one-piece guide design, it may not always be sufficient to maintain its position unaided. Therefore, we recommend that, when necessary, the guide stent be held manually while operating to stabilize it against dislodging forces. Metal material is recommended for printing, because it presents better mechanical properties [23] and dimensional stability [24] compared to light-polymerizing resin, which are imperative for the successful

application of guide system with fine structures. Although metal printing requires expensive equipment, the cost of external metal printing service is affordable nowadays and should be further reduced following the continuous technological innovation of metal printing in the future [25].

The specially designed experimental model with standard cylinders was applied in this study. This ensured that the models used for the freehand and guided groups were exactly the same, thereby eliminating the influence of sample heterogeneity that exists in traditional *in vitro* studies with extracted teeth. Moreover, application of this standardized model provides a new approach to calculate deviations using optimal scanning and 3D graphics analysis, which is more accurate, convenient, and safer than the traditional method using CBCT examination and measurement. One limitation of this *in vitro* study design was that different experiences may occur while drilling the printed homogeneous cylinder and the real fiber post within a dental root, which affects the face validity of the fiber post removal simulation. Nevertheless, this concern does not impact evaluation of the accuracy of this novel guide system, which is the primary objective of this study. Another limitation is that the experimental design does not facilitate blinding of the operator, which may add bias to the results, especially for the freehand group. To reduce this influence, the operator was not permitted to evaluate the drilling effect during the task to prevent the intentional correction. Besides, the operator bias should not affect the results of the guided group. Owing to the limitations of the *in vitro* design, the absolute deviation data should be carefully interpreted for clinical application. In the clinical setting, the accuracy can be influenced by additional factors such as precision of the data alignment, movement of the soft tissue, and the range of mouth opening. *In vivo* evaluation of the accuracy, safety, and efficiency under clinical conditions compared with the traditional endodontic revision approach using a dental microscope is required before general application of this novel guide technique.

## 5. Conclusions

Within the limits of an *in vitro* design, the accuracy of drilling with the novel 3D printed assembled sleeveless guide system used for fiber post removal is superior to that of the freehand method. Further clinical trials are required to evaluate this novel guide system under *in vivo* conditions.

## Funding

This work is supported by National Natural Science Foundation of China (82170982), National Multidisciplinary Cooperative Diagnosis and Treatment Capacity Building Project for Major Diseases (PKUSSNMP-201901) and Program for New Clinical Techniques and Therapies of Peking University School and Hospital of Stomatology (PKUSSNCT-22B10).

## CRedit authorship contribution statement

**Siyi Mo:** Investigation, Writing – original draft. **Yongwei Xu:** Investigation, Formal analysis, Writing – review & editing. **Lei Zhang:** Supervision, Writing – review & editing. **Ye Cao:** Methodology, Supervision, Writing – review & editing. **Yongsheng Zhou:** Supervision, Writing – review & editing. **Xiaoxiang Xu:** Conceptualization, Methodology, Writing – review & editing.

## Declaration of Competing Interest

The authors declare that they have no known competing financial interests or personal relationships that could have appeared to influence the work reported in this paper.

## Acknowledgments

The authors thank Lu Jia from Dental Laboratory of Peking University School and Hospital of Stomatology for technical assistance. This work is supported by National Natural Science Foundation of China (82170982), National Multidisciplinary Cooperative Diagnosis and Treatment Capacity Building Project for Major Diseases (PKUSSNMP-201901) and Program for New Clinical Techniques and Therapies of Peking University School and Hospital of Stomatology (PKUSSNCT-22B10).

## References

- [1] M.C. Cagidiaco, C. Goracci, F. Garcia-Godoy, M. Ferrari, Clinical studies of fiber posts: a literature review, *Int. J. Prosthodont.* 21 (4) (2008) 328–336.
- [2] G.C. Anderson, J. Perdigão, J.S. Hodges, W.R. Bowles, Efficiency and effectiveness of fiber post removal using 3 techniques, *Quintessence Int.* 38 (8) (2007) 663–670.
- [3] T. Castriso, P.V. Abbott, A survey of methods used for post removal in specialist endodontic practice, *Int. Endod. J.* 35 (2) (2002) 172–180.
- [4] M. Lindemann, P. Yaman, J.B. Dennison, A.A. Herrero, Comparison of the efficiency and effectiveness of various techniques for removal of fiber posts, *J. Endod.* 31 (7) (2005) 520–522.
- [5] J.H. Altshul, G. Marshall, L.A. Morgan, J.C. Baumgartner, Comparison of dental crack incidence and of post removal time resulting from post removal by ultrasonic or mechanical force, *J. Endod.* 23 (11) (1997) 683–686.
- [6] S. Aydemir, G. Arukaslan, S. Sarıdağ, I. Kaya-Büyükbayram, Y. Ylıdıran, Comparing fracture resistance and the time required for two different fiber post removal systems, *J. Prosthodont.* 27 (8) (2018) 771–774.
- [7] D. Çapar İ, B. Uysal, E. Ok, H. Arslan, Effect of the size of the apical enlargement with rotary instruments, single-cone filling, post space preparation with drills, fiber post removal, and root canal filling removal on apical crack initiation and propagation, *J. Endod.* 41 (2) (2015) 253–256.
- [8] F. Haupt, J. Pfitzner, M. Hülsmann, A comparative *in vitro* study of different techniques for removal of fibre posts from root canals, *Aust. Endod. J.* 44 (3) (2018) 245–250.
- [9] F. Schwendicke, Digital dentistry: advances and challenges, *J. Clin. Med.* 9 (12) (2020) 4005.
- [10] J. D'Haese, J. Ackhurst, D. Wismeijer, H. De Bruyn, A. Tahmaseb, Current state of the art of computer-guided implant surgery, *Periodontol* 73 (1) (2000) 121–133 (2017).
- [11] T. Connert, R. Weiger, G. Krastl, Present status and future directions - guided endodontics, *Int. Endod. J.* (2022).
- [12] C. Cho, H.J. Jo, J.H. Ha, Fiber-reinforced composite post removal using guided endodontics: a case report, *Restor. Dent. Endod.* 46 (4) (2021) e50.
- [13] L.M. Maia, G. Moreira Junior, R.C. Albuquerque, V. de Carvalho Machado, N. da Silva, D.D. Hauss, R.R. da Silveira, Three-dimensional endodontic guide for adhesive fiber post removal: a dental technique, *J. Prosthet. Dent.* 121 (3) (2019) 387–390.
- [14] C. Perez, G. Finelle, C. Couvrechel, Optimisation of a guided endodontics protocol for removal of fibre-reinforced posts, *Aust. Endod. J.* 46 (1) (2020) 107–114.
- [15] F.S. Schwindling, A. Tasaka, T. Hilgenfeld, P. Rammelsberg, A. Zenthöfer, Three-dimensional-guided removal and preparation of dental root posts-concept and feasibility, *J. Prosthodont. Res.* 64 (1) (2020) 104–108.
- [16] S.J. Kwon, Y.J. Park, S.H. Jun, J.S. Ahn, I.B. Lee, B.H. Cho, H.H. Son, D.G. Seo, Thermal irritation of teeth during dental treatment procedures, *Restor. Dent. Endod.* 38 (3) (2013) 105–112.
- [17] F. Faul, E. Erdfelder, A.G. Lang, A. Buchner, G\*Power 3: a flexible statistical power analysis program for the social, behavioral, and biomedical sciences, *Behav. Res. Methods* 39 (2) (2007) 175–191.
- [18] Y. Su, C. Chen, C. Lin, H. Lee, K. Chen, Y. Lin, F. Chuang, Guided endodontics: accuracy of access cavity preparation and discrimination of angular and linear deviation on canal accessing ability-an *ex vivo* study, *BMC Oral Health* 21 (1) (2021) 606.
- [19] F. Bover-Ramos, J. Viña-Almunia, J. Cervera-Ballester, M. Peñarocha-Diogo, B. Garcia-Mira, Accuracy of implant placement with computer-guided surgery: a systematic review and meta-analysis comparing cadaver, clinical, and *in vitro* studies, *Int. J. Oral Maxillofac. Implants* 33 (1) (2018) 101–115.
- [20] C. Moreno-Rabie, A. Torres, P. Lambrechts, R. Jacobs, Clinical applications, accuracy and limitations of guided endodontics: a systematic review, *Int. Endod. J.* 53 (2) (2020) 214–231.
- [21] A. Tahmaseb, V. Wu, D. Wismeijer, W. Coucke, C. Evans, The accuracy of static computer-aided implant surgery: a systematic review and meta-analysis, *Clin. Oral Implan. Res.* 29 (S16) (2018) 416–435.
- [22] J. Mouhyi, M.A. Salama, F.G. Mangano, C. Mangano, B. Margiani, O. Admakin, A novel guided surgery system with a sleeveless open frame structure: a retrospective clinical study on 38 partially edentulous patients with 1 year of follow-up, *BMC Oral Health* 19 (1) (2019) 253.

- [23] T.D. Ngo, A. Kashani, G. Imbalzano, K.T.Q. Nguyen, D. Hui, Additive manufacturing (3D printing): a review of materials, methods, applications and challenges, *Compos. Part B Eng.* 143 (2018) 172–196.
- [24] L. Chen, W.S. Lin, W.D. Polido, G.J. Eckert, D. Morton, Accuracy, reproducibility, and dimensional stability of additively manufactured surgical templates, *J. Prosthet. Dent.* 122 (3) (2019) 309–314.
- [25] L.F. Velásquez-García, Y. Kornbluth, M.L. Yarmush, Biomedical applications of metal 3D printing, *Annu. Rev. Biomed. Eng.* 23 (1) (2021) 307–338.